Carbohydrate Polymers 98 (2013) 784–792

Contents lists available at SciVerse ScienceDirect

Carbohydrate Polymers

journal homepage: www.elsevier.com/locate/carbpol

Characterization and bisphenol A adsorption capacity of β-cyclodextrin–carboxymethylcellulose-based hydrogels

Hiroyuki Kono*, Kenta Onishi, Taichi Nakamura

Department of Science and Engineering for Materials, Tomakomai National College of Technology, Nishikioka 443, Tomakomai, Hokkaido 059-1275, Japan

ARTICLE INFO

Article history:
Received 16 April 2013
Received in revised form 24 June 2013
Accepted 27 June 2013
Available online 5 July 2013

Keywords:
Carboxymethylcellulose
Cyclodextrin
Hydrogel beads
Adsorption
Bisphenol A

ABSTRACT

Novel hydrogel beads having molecular adsorption abilities were prepared from carboxymethylcellulose sodium salt (CMC) and β-cyclodextrin (β-CD) by suspension crosslinking, using ethylene glycol diglycidyl ether (EGDE) in basic medium as a crosslinking agent. FTIR and solid-state NMR spectroscopic analysis revealed that the amount of incorporated β-CD and crosslinking densities within the hydrogel bead structures are strongly dependent on the molar feed ratio of β-CD to CMC during preparation. The hydrogel beads showed water-swelling capacities of 70–200 mL/g-polymer, with decreases in capacity associated with increased amounts of β-CD incorporated in the gel structure. The hydrogel beads also showed a high adsorption capacity toward bisphenol A (BPA) in water. Batch BPA-adsorption experiments were analyzed employing Langmuir isotherm models; hydrogel bead adsorption isotherms for BPA could be fitted to the Langmuir model. The maximum BPA-adsorption among the prepared series of hydrogel beads amounted to 167 μmol g^{-1}.

1. Introduction

Cyclodextrins (CDs) are torus-shaped cyclic oligosaccharides composed of α-(1 → 4) linked D-glucopyranose with six, seven, and eight units, namely, α-CD, β-CD, and γ-CD, respectively (Hedges, 1998; Rekharsky & Inoue, 1998). The compounds are produced from the decomposition of starch by cyclodextrin gluconotransferase (Biwer, Antanikian, & Heinzle, 2002; Leemhuis, Kelly, & Dijkhuizen, 2010), and are shown to be nontoxic (Antlsperger & Schmid, 1996; Martin Dell Valle, 2004). Among CDs, β-CD and its derivatives have been widely developed in industry because of the proper inside cavity and lower production cost (Wind, Uitdehaag, Buitelaar, Dijkstra, & Dijkhuizen, 1998). A great deal of literature has demonstrated that CDs are easily complexed with many chemical species, including organic molecules (Aoki, Nishikawa, & Hattori, 2003; Crini & Morcellet, 2002; Crini et al., 1998; Crini, 2005), inorganic molecules (Brusseau, Wang, & Wang, 1997; Wang & Brusseau, 1995), biomolecules (Colton, Carbeck, Rao, & Whitesides, 1998; Cooper & McAuley-Hacht, 1993; Guo et al., 2010), and ions (Wang & Brusseau, 1995; Brusseau et al., 1997) within their cavities. The binding mechanisms are attributed to chemical bonds or weak intermolecular forces (Berthod, Li, & Armstrong, 1992).

The hydroxyl groups of CDs can undergo reactions such as etherification, esterification, reduction, and crosslinking to obtain derivatives with some special properties, such as high water solubility, ideal surface activity, and lower water absorption (Albers & Müller, 1996; Szente & Szejtli, 1999). Recently, polymerization of CDs has been explored as a highly effective technique for manipulating CD functionality and properties, such as stability toward heat, pH, shear forces, and insolubility (Crini & Morcellet, 2002; Crini et al., 1998; Crini, 2005). Among polymerized CDs, water-insoluble CD polymers have found use as a new type of adsorbent material useful for removal of organic pollutants and heavy metal ions in water (Cadars, Foray, Gadelle, Gerbaud, & Bardet, 2005; Gerbaud, Hediger, Gadelle, & Bardet, 2008; Gu, Tsai, & Tsao, 2006; Harada, Furue, & Nozakura, 1981; Kitaoka & Hayashi, 2002; Sreenivasan, 1996; Werner, Iannacone, & Amoo, 1996). The general method to obtain water-insoluble CD polymers is through crosslinking of CD molecules by use of bifunctional crosslinking agents. Epichlorohydrin (ECH) is the most popularly and extensively used reagent to produce CD polymeric materials, with water-insoluble CD polymers being obtained by treatment with ECH in a concentrated sodium hydroxide (NaOH) solution (Cadars et al., 2005; Gerbaud et al., 2008; Gu et al., 2006; Harada et al., 1981; Kitaoka & Hayashi, 2002; Sreenivasan, 1996; Werner et al., 1996). However, ECH produces a large amount of poisonous and carcinogenic byproducts under the strong alkaline conditions required for reaction (Wester, van der Heijden, Bisschop, & van Esch, 1985), and the CD polymers

Abbreviations: AGU, anhydroglucose unit; BPA, bisphenol A; CD, cyclodextrin; CMC, sodium carboxymethylcellulose; DS, degree of substitution; ECH, epichlorohydrin; EGDE, ethylene glycol diglycidyl ether; FTIR, Fourier transform infrared spectroscopy; NMR, nuclear magnetic resonance.

* Corresponding author. Tel.: +81 144 67 8036; fax: +81 144 67 8036.
E-mail address: kono@sem.tomakomai-ct.ac.jp (H. Kono).

0144-8617/$ – see front matter © 2013 Elsevier Ltd. All rights reserved.
http://dx.doi.org/10.1016/j.carbpol.2013.06.065

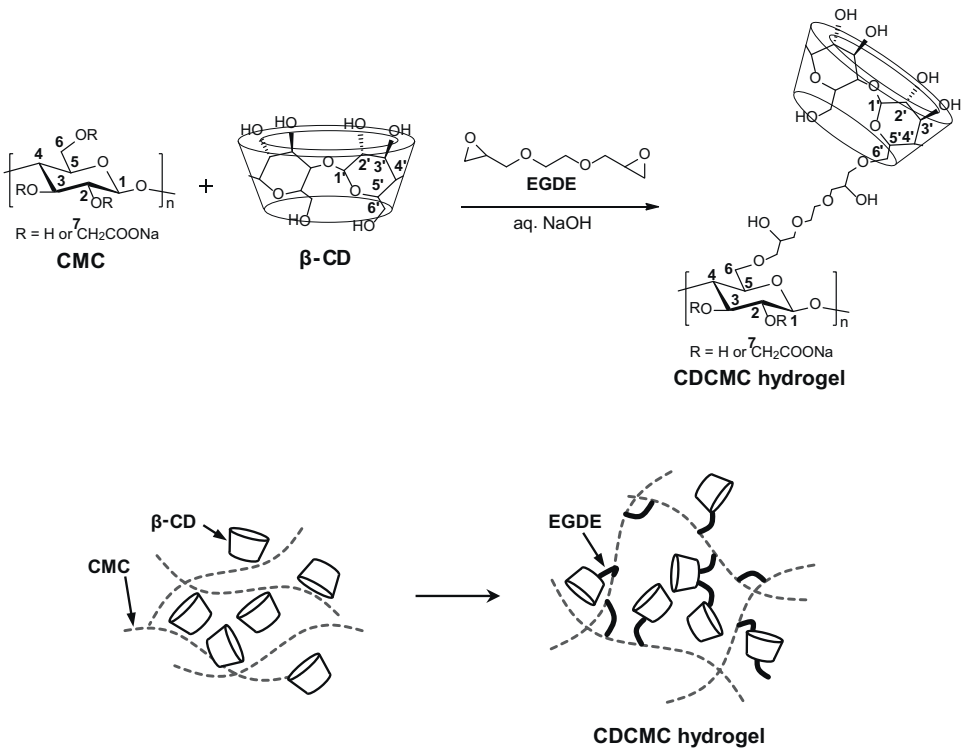

Fig. 1. Scheme for CDCMC hydrogel bead synthesis via polymerization of β-CD and CMC (top), and schematic illustration of the formation of the CMC hydrogel beads from β-CD and CMC (bottom). In the top figure, the linkage positions of CMC and β-CD are shown at C6 and C6′, respectively. EGDE also can react with two hydroxyl groups of the other position of CMC and β-CD to form cross-linked linkages, which was omitted in this figure.

obtained through this method have poor physical properties in general (Szente & Szejtli, 2004). As a consequence, compression, deformation, and cracking of CD polymers frequently occur during use.

Carboxymethylcellulose sodium salt (CMC), which is obtained from the reaction of hydroxyl groups at the 2, 3, and 6 positions of the anhydroglucose units (AGUs) of cellulose with chloroacetic acid, is an important water-soluble cellulose ether used in the fields of food, cosmetics, and paint as a viscosity modifier, thickener, emulsion stabilizer, and water-retention agent. CMC also has tremendous potential for use in pharmaceutical products such as site-specific or controlled-release drug delivery system carrier matrices due to its high biocompatibility, biodegradability, and low immunogenicity (Colombo, Bettini, Sabti, & Peppas, 2000; Ugwoke, Kaufmann, Verbeke, & Kinget, 2000). Crosslinking CMC has also been accomplished by bifunctional crosslinking agents such as ECH (Chang, Duan, Cai, & Zhang, 2010), diepoxy (Lin, Kumar, Rozman, & Noor, 2005; Rodfiguez, Alvarez-Lorenzo, & Concheiro, 2003), and dicarboxylic acid compounds (Akar, Antinişk, & Seki, 2012); the crosslinked CMC generally absorbs large amounts of water, swelling to form the hydrogel with excellent physical properties in dynamic viscoelasticity (Nerurkar, Elliott, & Mauck, 2010). Therefore, development of a polymerization method for CD and CMC hydrogel materials that retain the model encapsulation abilities of CDs is desired. Furthermore, it is envisioned that materials prepared through optimized methods would possess the advantages of a CMC hydrogel framework, without the less-than-ideal physical properties typically observed of CD polymers. In addition, such hydrogels may possess the potential for new applications as functional soft materials.

In this paper, we report on the preparation of new β-CD-incorporated CMC (CDCMC) hydrogel beads from CMC and β-CD with ethylene glycol diglycidyl ether (EGDE) as a crosslinking agent, as shown in Fig. 1. By changing the feed ratio of β-CD to CMC, a series of CDCMC beads were prepared using a suspension crosslinking method. Structural characterization of the new materials was performed using FTIR, solid-state NMR, and binocular wide-field dissecting and scanning electron microscopy. In addition, in order to confirm the encapsulation ability of CDCMC hydrogel beads, a preliminary study on adsorption of bisphenol A (BPA), a well-known endocrine-disrupting chemical (von Saal, Nagel, Coe, Angle, & Taylor, 2012), was conducted, the results of which is also described herein.

2. Experimental

2.1. Materials

Commercial β-CD (purity 99.4%), CMC (average degree of polymerization; 500) with a degree of substitution (DS) of 0.68, and BPA were purchased from Wako Pure Chemical Industries, Ltd. (Japan). EGDE was purchased from Tokyo Chemical Industry Co., Ltd. (Japan). All solvents and other chemicals (analytical grade) were purchased from Kanto Chemical Co. Inc. (Japan).

2.2. Preparation of CDCMC hydrogel beads

In this study, four types of CDCMC hydrogel beads (entries **1**–**4**) and CMC hydrogel beads (entry **5**) were prepared by inverse suspension crosslinking. A typical procedure to prepare the hydrogel beads is as follows: 5.0 g of CMC (23 mmol for monomer unit) and 3.7 g of β-CD (3.3 mmol) were dissolved in 1.5 mol L^{-1} aqueous NaOH. Next, 16 g of EGDE (92 mmol) was added to the solution with stirring at 300 rpm using a Teflon impeller at 30 °C. After 20 min, 300 mL of fluid wax (density: 0.87–0.90, flush point: 226 °C) was added to the reaction mixture. The inverse suspension crosslinking reaction of CMC and β-CD was held at 30 °C with stirring at 300 rpm for 12 h. The resulting beads were washed with n-heptane

Table 1
Additive amounts of CMC, β-CD, and EGDE for the preparation of CDCMC hydrogel beads (entries **1**–**4**) and CMC hydrogel beads (entry **5**) as a reference sample, and the yields of these hydrogel beads.

Entry	Initial additive amounts			Molar feed ratio of CMC and β-CD		Yields[e]
	CMC (AGU_{CMC})[a]	β-CD (AGU_{CD})[a]	EGDE[b]	AGU_{CMC}:AGU_{CD}[c]	AGU_{CMC}:β-CD[d]	
1	5.0 g (23 mmol)	3.7 g (23 mmol)	16.0 g (92 mmol)	1:1	7:1	15.8 g (74%)
2	2.5 g (11.5 mmol)	5.6 g (34.5 mmol)	16.0 g (92 mmol)	1:3	7:3	16.2 g (78%)
3	1.6 g (7.7 mmol)	6.2 g (38 mmol)	16.0 g (92 mmol)	1:5	7:5	15.9 g (78%)
4	1.2 g (5.8 mmol)	6.5 g (40 mmol)	16.0 g (92 mmol)	1:7	7:7	15.6 g (77%)
5	9.8 g (46 mmol)	0 g	16.0 g (92 mmol)			17.6 g (78%)

[a] AGU_{CMC} and AGU_{CD} are molar quantities of AGUs of CMC and β-CD added to the reaction mixture, respectively. For all entries, sum of AGU_{CMC} and AGU_{CD} was set to 46 mmol.
[b] Molar quantities of EGDE added to the reaction mixture, which was set to 92 mmol for all entries.
[c] Molar feed ratio of AGU_{CD} and AGU_{CMC} in the preparation of each hydrogel beads.
[d] Molar feed ratio of AGU_{CMC} and β-CD. For example, 7:1 (entry **1**) indicates that 1 mole of β-CD can react with 7 moles of AGUs in CMC.
[e] Yield (%) of each entry was determined by the following equation, (mass of hydrogel/g) × 100/[(sum of the mass of CMC, β-CD, and EGDE/g) − (2 × 92 mmol × 18 g/mol)]%. In this equation, yields were calculated on the assumption that all epoxy groups of EGDE molecules added to each reaction mixture were reacted with the hydroxyl groups of CMC and/or β-CD to form the ether linkages.

until fluid wax was completely removed. The beads were further washed with a deionized water and acetone solution (1:1, v/v) until unreacted materials were completely removed. Finally, the CDCMC hydrogel beads (entry **1**) were obtained after drying at 40 °C under reduced pressure. Using a similar method to prepare the CDCMC hydrogel beads (entry **1**), the other CDCMC hydrogel beads (entries **2**–**4**) and a CMC hydrogel bead sample (entry **5** used as a reference) were prepared. The additive amounts of the CMC, β-CD, and EGDE for the preparation of these hydrogel beads are listed in Table 1. All hydrogel beads were stored in a desiccator under vacuum until ready for use.

2.3. Structural analysis

2.3.1. FTIR spectroscopy

The FTIR spectra of the hydrogel beads were measured using a PerkinElmer Spectrum Two spectrometer (PerkinElmer Inc., US). FTIR spectra were recorded after grinding the sample into a powder and mixing well with KBr powder. The powder mixture was compressed into a transparent disk and scanned from 4000 to 400 cm^{-1} using an average of 16 scans, with a resolution of 1 cm^{-1}.

2.3.2. Solid-state NMR spectroscopy

Solid-state ^{13}C NMR spectra were recorded at 25 °C on a Bruker Biospin AVIII 500 spectrometer (BrukerBiospin Co., Ltd., Germany, ^{1}H frequency of 500 MHz) with a 4 mm dual-tuned MAS probe at a MAS frequency of 10 kHz. Dipolar-decoupled/magic angle spinning (DD/MAS) ^{13}C NMR experiments were performed on the hydrogel beads for quantitative analysis of the NMR spectra. ^{13}C-excitation pulse length (flip angle of 30°), data acquisition time, and repetition time were set to 1.5 μs, 20 ms, and 20 s, respectively. During the data acquisition period, SPINAL-64 (small phase incremental alternation with 64 steps) proton decoupling (Fung, Khitrin, & Ermolaev, 2000) was applied with ^{1}H field strength of 100 kHz. The spectra were typically accumulated 3076 scans to achieve an acceptable signal-to-noise ratio. ^{13}C chemical shifts of the spectra were calibrated based upon the carbonyl carbon resonance of D-glycine at 176.03 ppm, which was used as an external reference.

2.4. Morphological observation

Morphologies of both dried and swollen hydrogel beads at equilibrium were observed using an Olympus SZX-16 binocular wide-field dissecting microscope (Olympus Co., Japan) without pretreatment. Scanning electron microscope (SEM) images of the surface and cross-sectional structures of the swollen hydrogel beads were observed following sample preparation by the method as follows: after swelling in deionized water at 25 °C for 48 h, the hydrogel beads were carefully cut by use of razor blade, frozen to −70 °C, and then the freeze-dried under vacuum until water was sublimed. The freeze-dried sample was fixed on a specimen stubs sputter-coated with gold (Au) prior to observation. SEM images of the swollen gel beads were obtained by use of JEOL JSM 6330F scanning electron microscope (JEOL Ltd., Japan) with a potential of 1 kV.

2.5. Water absorbency

The water absorbency of the hydrogel beads were determined by the following method. Dried hydrogel beads (200 mg) were swollen in deionized water or the desired solution at 25 °C for 48 h. The swollen hydrogels at equilibrium were centrifuged at 15,000 rpm for 5 min, and the supernatant liquid solution was immediately drained. The weight of the swollen hydrogels (W_s) was measured, and the water absorbency was calculated using Eq. (1) (Kono & Fujita, 2012; Kono & Zakimi, 2013; Kono, Fujita, & Oeda, 2013).

$$\text{Water absorbency } (\%) = \frac{(W_s - W_d)}{W_d} \times 100 \quad (1)$$

where W_d is the weight of the dried hydrogel. As an external solution for determining the absorbency, distilled water and 50 mM citric acid–sodium citrate (pH 3), 50 mM NaH_2PO_4–Na_2HPO_4 (pH 7), and 50 mM glycine–NaOH (pH 10) buffer systems were used. These absorbency measurements were taken for five samples of each hydrogel beads.

2.6. BPA adsorption behavior

Dried hydrogel beads (20 mg) were placed into a 50 mL centrifuge tube containing 20 mL of 0.1 mM aqueous BPA solution, and then the tube was placed in a shaker at 25 °C (oscillation of 120 rpm). At different time intervals, the mixture was filtered by use of membrane filter with a pore size of 0.45 μm. BPA concentration of the filtrate was determined using a Thermo Fisher Scientific Evolution 201 UV-vis spectrophotometer (Thermo Fisher Scientific Inc., US) at the wavelength of 275 nm and using an earlier prepared calibration curve. The BPA adsorption capacity (q) of hydrogel beads was calculated using Eq. (2).

$$q_t = \frac{V(C_0 - C_t)}{W}, \quad (2)$$

where q_t (μmol g^{-1}) is the adsorption capacity at contact time t, V is the volume of BPA solution (L), C_0 is initial concentration of BPA (μmol L^{-1}), C_t is the concentration of BPA at contact time t (μmol L^{-1}), and W is the weight of hydrogel beads (g). The effects of

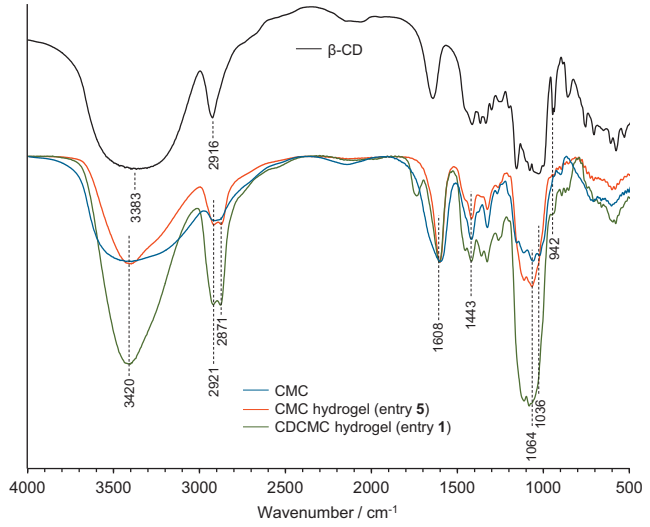

Fig. 2. FTIR spectra of β-CD, CMC, CMC hydrogel beads (entry **5**) and CDCMC hydrogel beads (entry **1**). The FTIR spectra of CMC, CMC hydrogel beads (entry **5**), and CDCMC hydrogel beads (entry **1**) were normalized by the peak intensity at 1608 cm^{-1}.

contact time and BPA concentration on the BPA adsorption capacity of each hydrogel beads were studied.

3. Results and discussion

3.1. Preparation of CDCMC hydrogel beads

CDCMC hydrogel beads were prepared from CMC and β-CD using a suspension crosslinking method with EGDE as a crosslinking agent in aqueous alkaline conditions. EGDE is a well-known reagent used for the crosslinking of polysaccharides via etherification reaction of hydroxyl groups. In the reaction, the two epoxy moieties of EGDE undergo successive nucleophilic attacks by two equivalents of an alkoxy anionic polysaccharide species generated under the basic conditions, thus forming the ether crosslinkage (Rodfiguez et al., 2003). In this study, as shown in Fig. 1, crosslinking reactions of CMC and β-CD were performed in order to obtain hydrogel beads possessing encapsulation abilities similar to that of β-CDs. As summarized in Table 1, a series of CDCMC hydrogel beads (entries **1**–**4**) were prepared by changing the molar feed ratio of β-CD to CMC to compare water-swelling behavior and encapsulation ability. CMC hydrogel beads were also prepared from CMC by similar method to prepare as an entry **5** to serve as a reference sample. All hydrogel beads were obtained as white granulous particles with diameters of approximately 0.4–1.2 mm.

3.2. FTIR analysis

FTIR spectra of β-CD, CMC itself, CMC hydrogel beads (entry **5**), and CDCMC hydrogel beads (entry **1**) are shown in Fig. 2. The spectra of starting CMC and both CMC and CDCMC hydrogel beads display common adsorption bands at 3420, 2921, 1608, 1443, and 1036 cm^{-1}, assigned to the stretching vibration of O—H, aliphatic C—H, asymmetric COO^-, symmetric COO^-, and bending of C—C, respectively (Barbucci, Magnani, & Consumi, 2000). The adsorption bands at 1608 and 1443 cm^{-1} in the CDCMC hydrogel beads indicate the presence of carbonyl groups within the CDCMC hydrogel framework after crosslinking. Compared with the spectrum of CMC, the new absorption bands at 2871 and 1064 cm^{-1} were observed in the spectra of both CMC and CDCMC hydrogel beads, with respective bands assigned to the bending vibration of C—H and

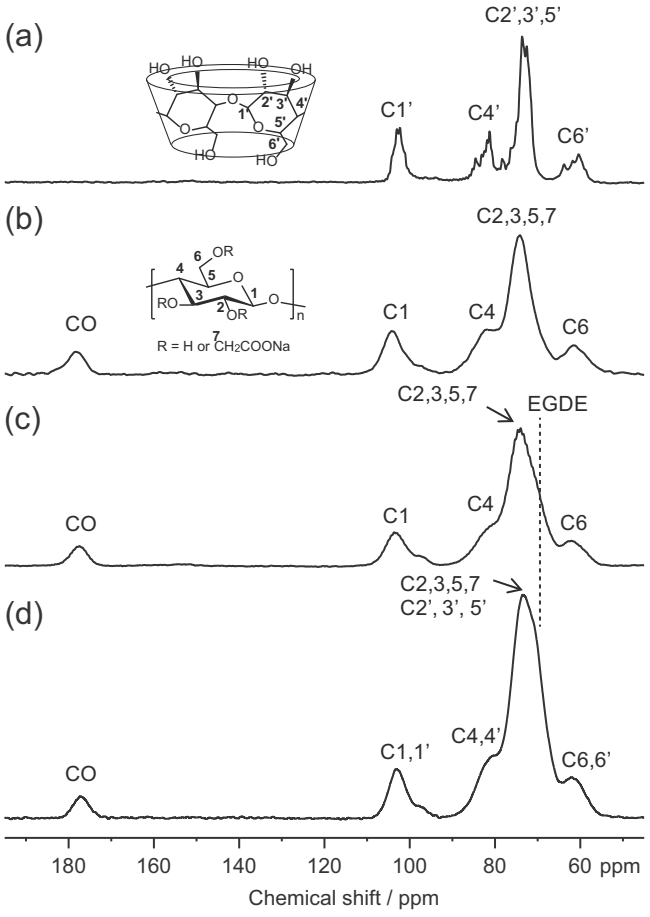

Fig. 3. Solid-state dipolar-decoupled/magic angle spinning (DD/MAS) ^{13}C nuclear magnetic resonance (NMR) spectra of (a) β-CD, (b) CMC, (c) CMC hydrogel beads (entry **5**), and (d) CDCMC hydrogel beads (entry **1**). The DD/MAS ^{13}C NMR spectra of (b) CMC, (c) CMC hydrogel beads (entry **5**), and (d) CDCMC hydrogel beads (entry **1**) were normalized by the peak intensity at 178 ppm.

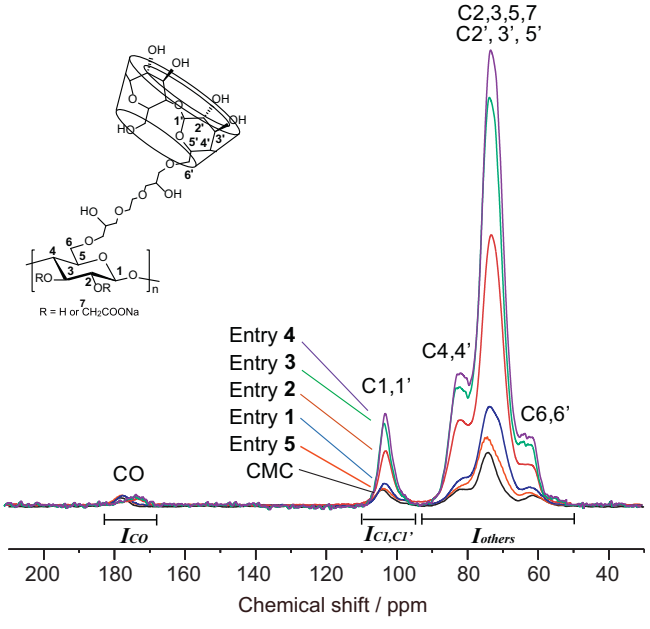

Fig. 4. Solid-state dipolar-decoupled/magic angle spinning (DD/MAS) ^{13}C nuclear magnetic resonance (NMR) spectra of CDCMC hydrogel beads (entries **1**–**4**), CMC hydrogel beads (entry **5**), and CMC starting material. The DD/MAS ^{13}C NMR spectra were normalized by the peak intensity of carbonyl carbons.

Table 2
Integrated values of ^{13}C resonances for CDCMC hydrogel beads (entries **1**–**4**), CMC hydrogel beads (entry **5**), and the starting material of CMC, and the structural parameters (n_{CD} and n_{EGDE}) of these hydrogel beads derived from the integrated values.

Entry	Integrated values of ^{13}C resonances			Structural parameters	
	I_{CO}[a]	$I_{C1,C1'}$[a]	I_{others}[a]	n_{CD}[b]	n_{EGDE}[c]
1	0.68	1.5	10	0.072	0.31
2	0.68	2.2	18	0.17	0.88
3	0.68	4.7	36	0.53	1.6
4	0.68	4.9	40	0.56	1.9
5	0.68	1.0	6.8	0	0.22
CMC	0.68	1.0	5.1		

[a] Integrated values I_{CO}, $I_{C1,C1'}$, I_{others} were determined from the integration of the carbonyl carbon region (183–168 ppm), C1 and C1′ region (110–93 ppm), and the other carbon region (92–50 ppm) in each solid-state ^{13}C NMR spectrum shown in Fig. 4, respectively. For all entries, I_{CO} was set to 0.68 which is DS of the starting material CMC.
[b] Average number of β-CD molecules per one AGU of CMC in each hydrogel bead.
[c] Average number of EGDE molecules per one AGU of total CMC and β-CD.

bending vibration of C—C (Wan Nagh, Endud, & Mayanar, 2002). These two bands are considered to be attributed to the presence of EGDE molecules reacted with β-CD and CMC, indicating successful crosslinking reaction by the EGDE.

The difference between the spectrum of CDCMC hydrogel beads and that of CMC hydrogel beads could be observed at adsorption at 942 cm^{-1}. The absorption band at 942 cm^{-1} assigned to the vibration of α-(1 → 4) glucopyranose ring (Kemnitz & Ritter, 2012) of β-CD could be detected in the spectrum of CDCMC hydrogel beads while such absorption could not be observed in the spectrum of CMC hydrogel beads. This indicates that β-CD and CMC are crosslinked by EGDE in the structure of CDCMC hydrogels beads. In order to obtain more detailed and clear information about the molecular structure of CDCMC hydrogel beads, solid-state ^{13}C NMR measurements were performed.

3.3. Solid-state ^{13}C NMR analysis

Fig. 3 shows the solid-state ^{13}C NMR spectra of β-CD, CMC itself, CMC hydrogel beads (entry **5**), and CDCMC hydrogel beads (entry **1**). In these spectra, carbon atoms of anhydroglucose unit (AGU) in β-CD were designated by prime notation; accordingly, for the ^{13}C NMR spectrum of β-CD, C1′, C4′ and C6′ peaks appear in the regions encompassing 110–100, 88–82, and 67–58 ppm, respectively, and the remaining C2′, C3′, and C5′ peaks overlap in the region of 82–70 ppm. In the ^{13}C NMR spectrum of CMC, broad ^{13}C resonances at 178, 105, 87, 76 and 63 ppm were assigned to carbonyl carbon, C1, C4, overlap of C2, C3, C5 and methylene carbons of carboxymethyl groups, and C6, respectively. The weak and broad resonance appearing around 96 ppm was attributed to the C1 resonance of carboxymethylated AGU at C2 because etherification at

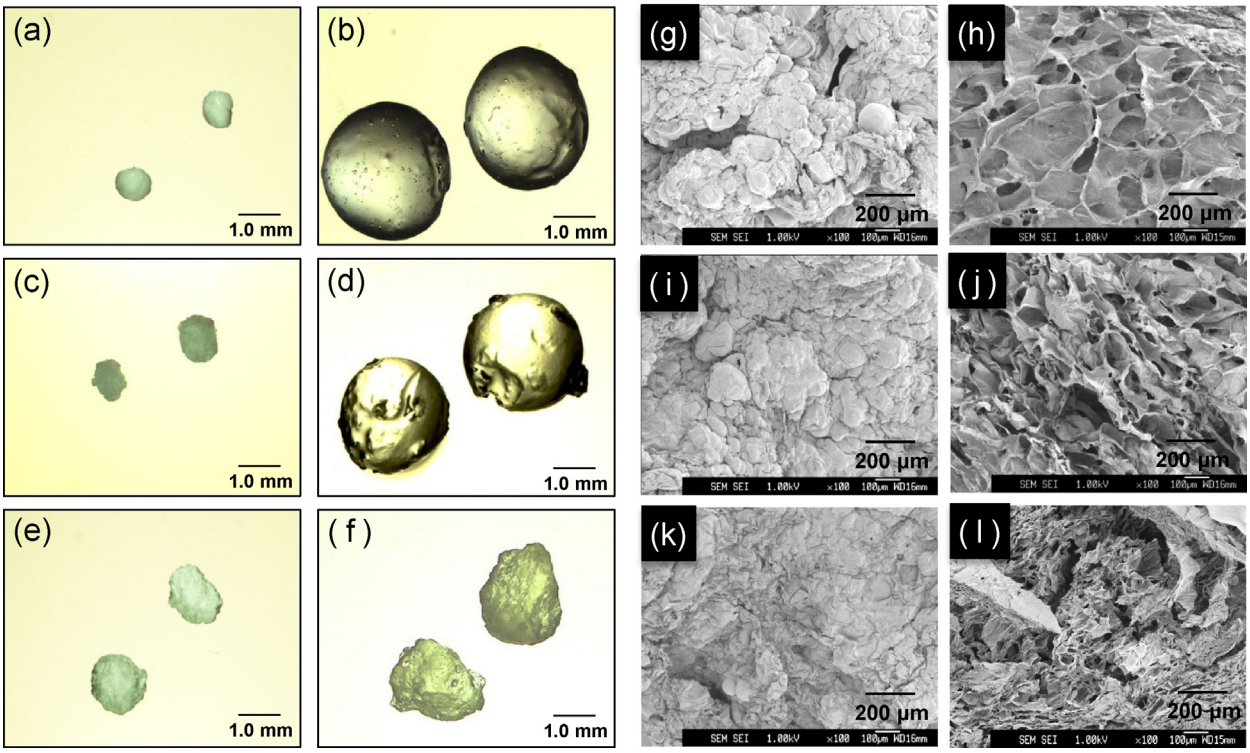

Fig. 5. Morphologies of CMC hydrogel beads (entry **5**) and CDCMC hydrogel beads (entries **1** and **4**). Binocular wide-field dissecting microscopic appearance (a)–(f): (a) dried and (b) swelled CMC hydrogel beads (entry **5**), (c) dried and (d) swelled CDCMC hydrogel beads (entry **1**), and (e) dried and (f) swelled CDCMC hydrogel beads (entry **4**). SEM images (g)–(l): (g) surface and (h) cross-section of CMC hydrogel beads (entry **5**), (i) surface and (j) cross-section of CDCMC hydrogel beads (entry **1**), and (k) surface and (l) cross-section of CDCMC hydrogel beads (entry **4**).

this position results in an upfield shift of about 5 ppm for C1 by β-effect of the substituent (Bubb, 2003). One of the notable differences between the spectrum of CMC and that of CMC hydrogel beads was in the intensity of the ^{13}C resonance at 96 ppm; the intensity of the signal in the hydrogel sample was greater in comparison with that of the starting material CMC. This indicates that the free hydroxyl group at C2 position of CMC underwent etherification with EGDE during hydrogel bead preparation. In addition, as indicated by the dotted line in Fig. 3, further evidence of a crosslinking reaction between CMC molecules by EGDE was confirmed with the appearance of a shoulder around 70 ppm which is attributed to the methylene carbons of EGDE (Denis et al., 2008). This distinct shoulder in the region of 70 ppm could be also observed in the spectrum of CDCMC hydrogels, suggesting that β-CD and CMC were also crosslinked by EGDE. The most notable spectral difference between the CMC and CDCMC hydrogel beads is the intensity of the ^{13}C resonances of the ring carbons and EGDE within the region of 110–50 ppm; the peak intensities of CDCMC were strongly enhanced in comparison with that of the CMC hydrogel – using peak intensity at 178 ppm as a reference – indicating that β-CD and CMC were in fact reacted with EGDE to form the hydrogel beads.

Fig. 4 shows the solid-state ^{13}C NMR spectra of the CDCMC hydrogels (entries **1**–**4**), CMC hydrogel beads (entry **5**), and CMC. An increase in signal intensities at 110–50 ppm in the CDCMC hydrogel beads was observed, becoming more pronounced with the increase in feed ratio of β-CD to CMC during hydrogel preparation; this increase in signal intensity is largely attributed to incorporation of β-CD molecules into the CMC hydrogel framework, with β-CD concentration directly proportional to the aforementioned molar feed ratio increase. For a quantitative discussion of β-CD incorporation as well as crosslinking density, the integral values of the carbonyl carbon resonances appearing in the region 183–168 ppm (I_{CO}), that of C1 and C1′ resonances appearing within 110–93 ppm ($I_{C1,C1'}$), and that of other ^{13}C resonances appearing in the region 92–50 ppm (I_{others}) were determined for each hydrogel, with results summarized in Table 2. From these integral values, the average number of β-CD per one AGU of CMC (n_{CD}) and average number of EGDE molecule per one AGU of total CMC and β-CD molecules (n_{EGDE}) could be determined by Eq. (3) and (4),

$$n_{CD} = \frac{I_{C1,C1'} - 1}{7} \quad (3)$$

$$n_{EGDE} = \frac{I_{other} - 5.68 - 5 \times (I_{C1,C1'} - 1)}{8}, \quad (4)$$

respectively, and these structural parameters n_{CD} and n_{EGDE} for each hydrogel are also summarized in Table 2. From this data, it was revealed that both n_{CD} and n_{EGDE} values are drastically increased with an increase in feed ratio of β-CD to CMC during CDCMC hydrogel bead preparation. The maximum n_{CD} value observed was 0.56 for the CDCMC hydrogel (entry **4**, Table 2). Although a reason for the accompanied increase of n_{EGDE} in CDCMC hydrogel beads with an increase in feed ratio could not be clearly characterized from the NMR and FTIR spectra, it is expected that EGDE not only served as a crosslinker between β-CD/CMC, β-CD/β-CD, and CMC/CMC, but also crosslinked between two hydroxyl groups in one β-CD molecule (intramolecular crosslinking).

3.4. Morphology and swelling behavior of CDCMC hydrogels

Fig. 5 (a)–(f) shows the morphologies of both CDCMC (entries **1** and **4**) and CMC hydrogel beads (entry **5**). The spherical white particles of these dried beads, possessing diameters of 0.4–1.2 mm, absorbed water readily, forming transparent hydrogels upon soaking. The diameter and transparency of the swelled CDCMC hydrogels depended once again on the feed ratio of β-CD to CMC,

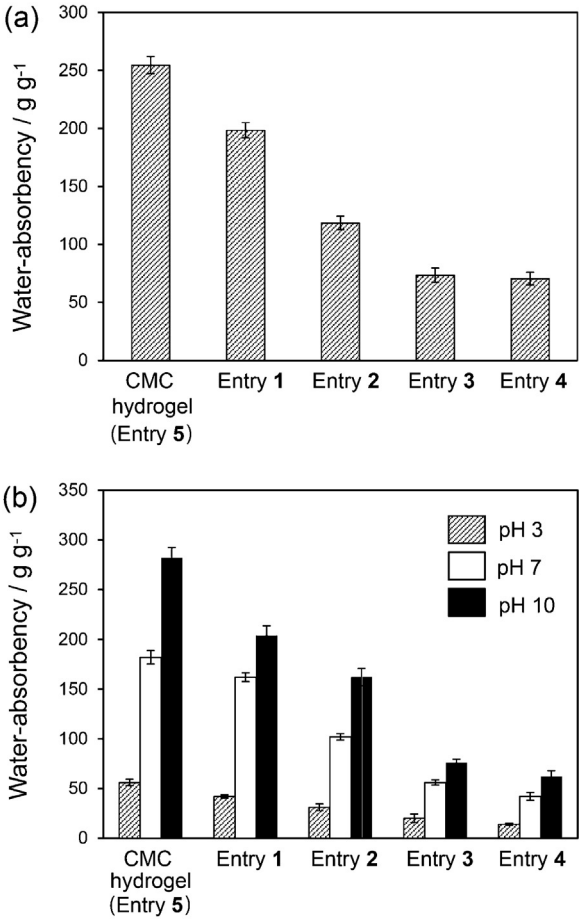

Fig. 6. Water absorbency of the CDCMC hydrogel beads (entries **1**–**4**) and CMC hydrogel beads (entry **5**) in deionized water (a) and in pH 3, 7, and 10 buffer solutions (b). The standard deviation value of each absorbency ($n = 5$) was shown in these figures.

with a reduction in diameter as well as transparency observed upon increase in feed ratio. A decrease in swelling of the CDCMC hydrogels accompanying increases in β-CD molecule incorporation was also confirmed through water absorbency experiments, as shown in Fig. 6(a), where the absorbencies of CDCMC hydrogel materials **1**–**4** in deionized water decreased to 78, 46, 29, and 28% compared to that of the CMC hydrogel (entry **5**) reference compound, respectively.

Fig. 5 (g)–(l) shows the SEM images of the surface and the cross-sections of the lyophilized CDCMC and CMC hydrogel beads. The surface of the CDCMC materials appear to be shrunk in comparison to that of CMC hydrogel beads. Furthermore, it could be clearly observed in the image of the cross-section surface that the bead pore size was reduced with an increase in β-CD feed ratio.

To confirm the electrostatic repulsions between carboxylate anions (COO^-) within the hydrogel network influence the hydrogel network expansion and the amount of water absorption, the absorbency of the CDCMC (entries **1**–**4**) and CMC hydrogel beads (entry **5**) under different pH buffer conditions were investigated. As shown in Fig. 6(b), effect of pH on the swelling behavior of the CDCMC hydrogel beads is similar to that of the CMC hydrogel beads. Absorbency of these hydrogel beads increased markedly with the increasing buffer pH due to the presence of carboxyl groups in the hydrogel structures. In the neutral and alkaline pH region, because the dominant charged species in these hydrogels are unprotonated carboxyl group, the hydrogels are swollen due to an intraionic repulsion between the unprotonated carboxyl groups. In the case

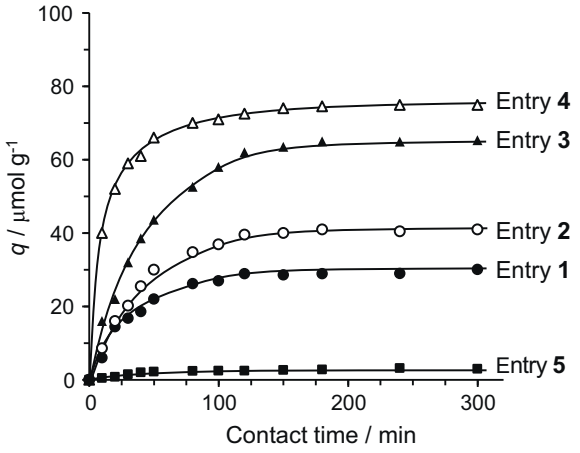

Fig. 7. BPA adsorption capacity (q) of CDCMC hydrogel beads (entries **1**–**4**) and CMC hydrogel beads (entry **5**). BPA adsorption measurements were performed under the following conditions: hydrogel bead content (dried): 20 mg; BPA initial concentration: 1.0 mmol L^{-1}; temperature: 25 °C; and volume of BPA solution: 20 mL.

of acidic pH, on the other hand, the carboxyl groups are protonated, thereby lowering the ionic repulsion, which causes the gels to shrink.

From these results, it is concluded that electrostatic repulsions between carboxylate anions between the hydrogel network – resulting in hydrogel network expansion and an increase in the amount of water absorption – decreased in proportion to greater amounts of incorporated β-CD units.

3.5. BPA adsorption capacity of CDCMC hydrogel beads

To confirm the encapsulation abilities of the prepared CDCMC hydrogel beads, adsorption behavior toward BPA was characterized. BPA has two phenolic functionalities, and its hydrophobic phenol group is known to be adsorbed within the hydrophobic cavity of β-CD (Aoki et al., 2003; Kitaoka & Hayashi, 2002). Fig. 7 shows the BPA adsorption capacity onto the CMC and CDCMC hydrogel beads as a function of contact time. Elevated adsorption rates were observed at the beginning of the adsorption experiments, as saturation was gradually achieved over the course of 180 min. The saturated amounts of BPA adsorbed after 300 min of contact time were 28.2, 38.4, 62.3, and 76.0 μmol g^{-1} (entries **1**–**4**, respectively), suggesting that BPA adsorption capacities strongly depend on the n_{CD} of the CDCMC hydrogel beads. CMC hydrogels also showed a very weak BPA adsorption capacity of 1.2 μmol g^{-1}. Because the CMC hydrogel beads are considered to have no or weak interactions with BPA molecules, CMC hydrogel beads seems to simply absorb water containing BPA into the network structure. This is a probable explanation since water absorbency of the CMC hydrogels is considerably higher than those of CDCMC hydrogel beads (Fig. 6(A)).

Fig. 8(a) shows the effect of the initial BPA concentration on the adsorption of BPA by the CDCMC hydrogel beads after 24 h. In the previous study of the BPA adsorption behavior of the

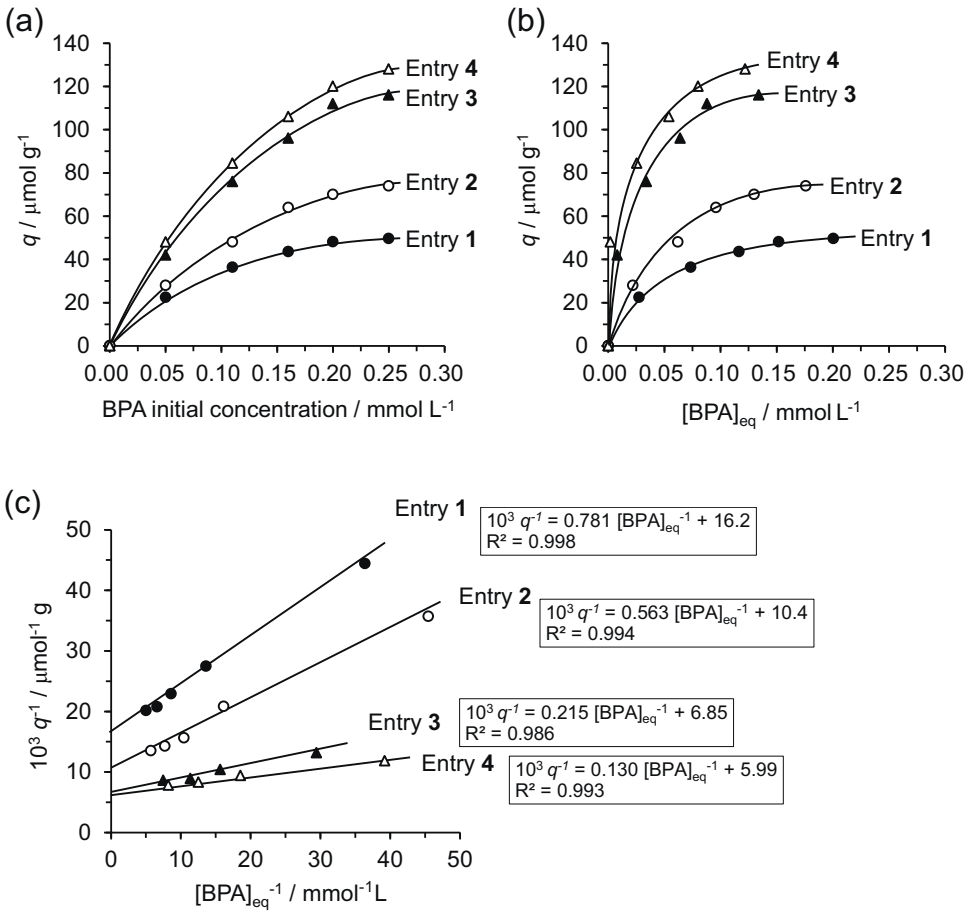

Fig. 8. (a) Effect of initial BPA concentration on BPA adsorption by CDCMC hydrogel beads (entries **1**–**4**). BPA adsorption was performed under the following conditions: hydrogel bead content (dried): 20 mg; temperature: 25 °C; contact time: 24 h; and volume of BPA solution: 20 mL. (b) Effect of $[BPA]_{eq}$ on BPA adsorption. (c) Linear representation of Langmuir-type adsorption of BPA on CDCMC hydrogel beads.

Table 3
Maximum adsorption capacity (q_m), the dissociation constant (K_d), and the equilibrium binding constant (K_b) for the BPA adsorption by CDCMC hydrogel beads determined by the Langmuir-type plot of the BPA adsorption systems (Fig. 8).

Entry	q_m (μmol g^{-1})	K_d (μmol L^{-1})	K_b (mol^{-1} L)
1	61.7	48.2	2.07×10^4
2	96.2	54.1	1.84×10^4
3	146	31.4	3.18×10^4
4	167	21.7	4.61×10^4

water-insoluble β-CD polymers prepared from the polymerization of β-CD with 1,2,3,4-butanetetracarboxylic dianhydride, it was revealed that the BPA adsorption by the β-CD polymers can be fitted by the Langmuir adsorption isotherm (Kono & Nakamura, 2013). Therefore, it was confirmed by use of the data shown in Fig. 8(a) that the Langmuir adsorption model could be applied to the BPA adsorption by the CDCMC hydrogels. In the Langmuir adsorption model, the maximum BPA adsorption capacity (q_m) of the CDCMC hydrogel and equilibrium binding constant (K_b) of the adsorption system can be described by the relation Eq. (5),

$$\frac{1}{q} = \frac{K_d}{q_m [BPA]_{eq}} + \frac{1}{q_m} \quad (5)$$

where q is the equilibrium adsorption capacity of BPA adsorbed on CDCMC hydrogel, q_m is the maximum adsorption capacity of the CDCMC, $[BPA]_{eq}$ is the BPA equilibrium concentration of the BPA solution, and K_d is the dissociation constant of the system (Chase, 1984; Kono & Nakamura, 2013; Kono, Oeda, & Nakamura, 2013). Fig. 8(b) shows the plot of the $[BPA]_{eq}$ vs. q. In this figure, concentration of the BPA solution after 24 h of contact time was used for the $[BPA]_{eq}$ because saturation of this system was achieved over the course of 180 min (Fig. 7). Finally, double reciprocal plots of q and $[BPA]_{eq}$ were performed for CDCMC hydrogel beads (Fig. 8(c)), and the adsorption isotherms of BPA for the CDCMC hydrogels are confirmed to be typical for Langmuir-type adsorption behavior which can be described by Eq. (5). Based on Fig. 8(c), it was revealed that q_m of CDCMC hydrogel beads (entries **1**–**4**) were 61.7, 96.2, 146, and 167 μmol g^{-1}, with dissociation constants K_d of 48.2, 54.1, 31.4, and 21.7 μmol L^{-1}, respectively (Table 3). Therefore, equilibrium binding constant K_b could be determined by Eq. (6)

$$K_b = \frac{1}{K_d} \quad (6)$$

As summarized in Table 3, K_b of CDCMC hydrogel beads (**1**–**4**) were 2.07×10^4, 1.84×10^4, 3.18×10^4, and 4.61×10^4 mol^{-1} L, respectively. This data indicates that CDCMC hydrogel beads forms stable inclusion complex with BPA at β-CD sites of the hydrogels. Thus, it is expected that CDCMC hydrogels may possibly combine with a variety of molecules such as organic and inorganic species, biomolecules, and ions in the cavities of the incorporated CD molecules.

4. Conclusions

Novel CMC-based hydrogel beads with β-CD encapsulation abilities were prepared from CMC and CD compounds, employing a suspension crosslinking method – utilizing EGDE as crosslinking agent – under alkaline conditions. The molar feed ratio of β-CD to CMC in the preparation of CDCMC hydrogel beads strongly influenced n_{CD} and n_{EGDE} of the obtained hydrogels. In addition, increase of n_{CD} was shown to lead to the decrease of hydrogel bead water absorbency, due in part to the diminished electrostatic repulsion effects of carboxylate moieties within the hydrogel framework. The CDCMC hydrogel beads exhibited good adsorption abilities toward BPA, with a maximum adsorption capacity of 167 μmol g^{-1}. The physical and chemical properties of the CDCMC hydrogel beads such as dynamic viscoelasticity, biodegradability, and adsorption capacity toward the other organic and inorganic compounds are currently under investigation; a full report of these studies will be provided in the near future.

Acknowledgments

This work was supported in part by Grants-in-Aid for Scientific Research C-25410134 from the Japan Society for Promotion of Science (JSPS), and Grants-in-aids for the Adaptable and Seamless Technology Transfer Program through Targetdrive R&D (241FT0160 and AS242Z03384M) and Grants-in-aids for the Promoting Patent Licensing form Universities and Public Research Institutions to Industries from Japan Science and Technology Agency (JST).

References

Akar, E., Antinişk, A., & Seki, Y. (2012). Preparation of pH- and ionic-strength responsive biodegradable fumaric acid crosslinked carboxymethyl cellulose. *Carbohydrate Polymers*, *90*, 1634–1641.
Albers, E., & Müller, B. W. (1996). Cyclodextrin derivatives in pharmaceutics. *Critical Reviews in Therapeutic Drug Carrier Systems*, *12*, 311–337.
Antlsperger, G., & Schmid, G. (1996). Toxicological comparison of cyclodextrins. In J. Szejtili, & L. Szente (Eds.), *Proceedings of the eighth international symposium on cyclodextrins* (pp. 149–155). Dordrecht: Kluwer Academic Publishers.
Aoki, N., Nishikawa, M., & Hattori, K. (2003). Synthesis of chitosan derivatives bearing cyclodextrin and adsorption of *p*-nonylphenol and bisphenol A. *Carbohydrate Polymers*, *52*, 219–223.
Barbucci, R., Magnani, A., & Consumi, M. (2000). Swelling behavior of carboxymethylcellulose hydrogels in relation to cross-linking, pH, and charge density. *Macromolecules*, *33*, 7475–7480.
Berthod, A., Li, W., & Armstrong, D. W. (1992). Multiple enantioselective retention mechanisms on derivatized cyclodextrin gas chromatographic chiral stationary phases. *Analytical Chemistry*, *64*, 873–879.
Biwer, A., Antranikian, G., & Heinzle, E. (2002). Enzymatic production of cyclodextrins. *Applied Microbiology and Biotechnology*, *59*, 609–617.
Brusseau, M. L., Wang, X., & Wang, W.-Z. (1997). Simultaneous elution of heavy metals and organic compounds from soil by cyclodextrin. *Environmental Science & Technology*, *31*, 1087–1092.
Bubb, W. A. (2003). NMR spectroscopy in the study of carbohydrates: Characterizing the structural complexity. *Concepts in Magnetic Resonance Part A*, *19A*(1), 1–19.
Cadars, S., Foray, M. F., Gadelle, A., Gerbaud, G., & Bardet, M. (2005). High-resolution solid-state ^{13}C NMR study of per(3,6-anhydro)-α-cyclodextrin based polymers and of their chromium complexes. *Carbohydrate Polymers*, *61*, 88–94.
Chang, C., Duan, B., Cai, J., & Zhang, L. (2010). Superabsorbent hydrogels based on cellulose for smart swelling and controllable delivery. *European Polymer Journal*, *46*, 92–100.
Chase, H. A. (1984). Prediction of the performance of preparative affinity chromatography. *Journal of Chromatography A*, *297*, 279–202.
Colombo, P., Bettini, R., Sabti, P., & Peppas, N. A. (2000). Swellable matrices for controlled drug delivery: Gel-layer behaviour, mechanisms and optimal performance. *Pharmaceutical Science & Technology Today*, *3*, 198–204.
Colton, I. J., Carbeck, J. D., Rao, J., & Whitesides, G. M. (1998). Affinity capillary electrophoresis: A physical-organic tool for studying interactions in biomolecular recognition. *Electrophoresis*, *19*, 367–382.
Cooper, A., & McAuley-Hacht, K. E. (1993). Microcalorimetry and the molecular recognition of peptides and proteins. *Philosophical Transactions of the Royal Society of London. Series A: Physical and Engineering Sciences*, *345*, 23–25.
Crini, G. (2005). Recent developments in polysaccharide-based materials used as adsorbents in wastewater treatment. *Progress in Polymer Science*, *30*, 38–70.
Crini, G., Bertini, S., Torri, G., Naggi, A., Sforzini, D., Vecchi, C., et al. (1998). Sorption of aromatic compounds in water using insoluble cyclodextrin polymers. *Journal of Applied Polymer Science*, *68*, 1973–1978.
Crini, G., & Morcellet, M. (2002). Synthesis and applications of adsorbents containing cyclodextrins. *Journal of Separation Science*, *25*, 789–813.
Denis, M. F. L., Carballo, R. R., Spiaggi, A. J., Dabas, P. C., Dall' Orto, V. C., Martínez, J. M. L., et al. (2008). Synthesis and sorption properties of a polyampholyte. *Reactive and Functional Polymers*, *68*, 169–181.
Fung, B. M., Khitrin, A. K., & Ermolaev, K. (2000). An improved broadband decoupling sequence for liquid crystals and solids. *Journal of Magnetic Resonance*, *142*, 97–101.
Gerbaud, G., Hediger, S., Gadelle, A., & Bardet, M. (2008). Synthesis and solid-state NMR study of chromium complexes of per(3,6-anhydro)-α-cyclodextrin based polymers. *Carbohydrate Polymers*, *73*, 64–73.
Gu, T., Tsai, G.-J., & Tsao, G. T. (2006). Synthesis of rigid cyclodextrin-containing polymeric resins for adsorption. *Journal of Inclusion Phenomena and Macrocyclic Chemistry*, *56*, 375–379.
Guo, Y., Guo, S., Ren, J., Zhai, Y., Dong, S., & Wang, E. (2010). Cyclodextrin functionalized graphene nanosheets with high supramolecular recognition capability:

Synthesis and host-guest inclusion for enhanced electrochemical performance. *ACS Nano*, *4*, 4001–4010.
Harada, A., Furue, M., & Nozakura, S.-I. (1981). Inclusion of aromatic compounds by a β-cyclodextrin-epichlorohydrin polymer. *Polymer Journal*, *13*, 777–781.
Hedges, A. R. (1998). Industrial applications of cyclodextrins. *Chemical Reviews*, *98*, 2035–2044.
Kemnitz, M., & Ritter, H. (2012). Influence of cyclodextrin on the solubility and the polymerization of (meth)acrylated Triton® X-100. *Beilstein Journal of Organic Chemistry*, *8*, 2176–2183.
Kitaoka, M., & Hayashi, K. (2002). Adsorption of bisphenol A by cross-linked β-cyclodextrin polymer. *Journal of Inclusion Phenomena and Macrocyclic Chemistry*, *44*, 429–431.
Kono, H., & Fujita, S. (2012). Biodegradable superabsorbent hydrogels derived from cellulose by esterification crosslinking with 1,2,3,4-butanetetracarboxylic dianhydride. *Carbohydrate Polymers*, *87*, 2582–2588.
Kono, H., Fujita, S., & Oeda, I. (2013). Comparative study of homogeneous solvents for the esterification crosslinking of cellulose with 1,2,3,4-butanetetracarboxylic dianhydride and water absorbency of the reaction products. *Journal of Applied Polymer Science*, *127*, 478–486.
Kono, H., & Nakamura, T. (2013). Polymerization of β-cyclodextrin with 1,2,3,4-butanetetracarboxylic dianhydride: Synthesis, structural characterization, and bisphenol A adsorption capacity. *Reactive and Functional Polymers*, *73*, 1096–1102.
Kono, H., Oeda, I., & Nakamura, T. (2013). The preparation, swelling characteristics, and albumin adsorption and release behaviors of a novel chitosan-based polyampholyte hydrogel. *Reactive and Functional Polymers*, *73*, 97–107.
Kono, H., & Zakimi, M. (2013). Preparation, water absorbency, and enzyme degradability of novel chitin- and cellulose/chitin-based superabsorbent hydrogels. *Journal of Applied Polymer Science*, *128*, 572–581.
Leemhuis, H., Kelly, R. M., & Dijkhuizen, L. (2010). Engineering of cyclodextrin glucanotransferases and the impact for biotechnological applications. *Applied Microbiology and Biotechnology*, *85*, 823–835.
Lin, O. H., Kumar, R. N., Rozman, H. D., & Noor, M. A. M. (2005). Grafting of sodium carboxymethyl cellulose (CMC) with glycidyl methacrylate and development of UV curable coatings from CMC-g-GMA induced by cationic photoinitiators. *Carbohydrate Polymers*, *69*, 57–69.
Martin Dell Valle, E. M. (2004). Cyclodextrins and their uses: A review. *Process Biochemistry*, *39*, 1033–1046.
Nerurkar, N. L., Elliott, D. M., & Mauck, R. L. (2010). Mechanical design criteria for intervertebral disc tissue engineering. *Journal of Biomechanics*, *43*, 1017–1030.
Rekharsky, M. V., & Inoue, Y. (1998). Complexation thermodynamics of cyclodextrins. *Chemical Reviews*, *98*, 1875–1918.
Rodŕiguez, R., Alvarez-Lorenzo, C., & Concheiro, A. (2003). Cationic cellulose hydrogels: Kinetics of the cross-linking process and characterization as pH-/ion-sensitive drug delivery systems. *Journal of Controlled Release*, *86*, 253–265.
Sreenivasan, K. (1996). Synthesis and characterization of poly (vinyl alcohol)-β-cyclodextrin copolymer. *Die Angewandte Makromolekulare Chemie*, *235*, 15–20.
Szente, L., & Szejtli, J. (1999). Highly soluble cyclodextrin derivatives: Chemistry, properties, and trends in development. *Advanced Drug Delivery Reviews*, *36*, 17–28.
Szente, L., & Szejtli, J. (2004). Cyclodextrins as food ingredients. *Trends in Food Science & Technology*, *15*, 137–142.
Ugwoke, M. I., Kaufmann, G., Verbeke, N., & Kinget, R. (2000). Intranasal bioavailability of apomorphine from carboxymethylcellulose-based drug delivery systems. *International Journal of Pharmaceutics*, *202*, 125–131.
von Saal, F. S., Nagel, S. C., Coe, B. L., Angle, B. M., & Taylor, J. A. (2012). The estrogenic endocrine disrupting chemical bisphenol A (BPA) and obesity. *Molecular and Cellular Endocrinology*, *354*, 74–84.
Wan Nagh, W. S., Endud, C. S., & Mayanar, R. (2002). Removal of copper(II) ions from aqueous solution onto chitosan and cross-linked chitosan beads. *Reactive and Functional Polymers*, *50*, 181–190.
Wang, X., & Brusseau, M. L. (1995). Simultaneous complexation of organic compounds and heavy metals by a modified cyclodextrin. *Environmental Science & Technology*, *29*, 2632–2635.
Werner, T. C., Iannacone, J. L., & Amoo, M. N. (1996). The binding of pyrene and other probes to CD polymers. *Journal of Inclusion Phenomena and Macrocyclic Chemistry*, *25*, 77–80.
Wester, P. W., van der Heijden, C. W., Bisschop, G. J., & van Esch, G. J. (1985). Carcinogenicity study with epichlorohydrin (CEP) by gavage in rats. *Toxicology*, *36*, 325–339.
Wind, R. D., Uitdehaag, J. C. M., Buitelaar, R. M., Dijkstra, B. W., & Dijkhuizen, L. (1998). Engineering of cyclodextrin product specificity and pH optima of the thermostable cyclodextrin glycosyltransferase from *Thermoanaerobacterium thermosulfurigenes* EM_1. *Journal of Biological Chemistry*, *273*, 5771–5779.